nature communications

Article

https://doi.org/10.1038/s41467-024-51449-9

Role of the Labrador Current in the Atlantic Meridional Overturning Circulation response to greenhouse warming

Received: 12 February 2024

Accepted: 6 August 2024

Published online: 27 August 2024

Check for updates

Xuan Shan[1,2] ✉, Shantong Sun[3] ✉, Lixin Wu[1,3] & Michael Spall[2]

Anthropogenic warming is projected to enhance Arctic freshwater exportation into the Labrador Sea. This extra freshwater may weaken deep convection and contribute to the Atlantic Meridional Overturning Circulation (AMOC) decline. Here, by analyzing an unprecedented high-resolution climate model simulation for the 21st century, we show that the Labrador Current strongly restricts the lateral spread of freshwater from the Arctic Ocean into the open ocean such that the freshwater input has a limited role in weakening the overturning circulation. In contrast, in the absence of a strong Labrador Current in a climate model with lower resolution, the extra freshwater is allowed to spread into the interior region and eventually shut down deep convection in the Labrador Sea. Given that the Labrador Sea overturning makes a significant contribution to the AMOC in many climate models, our results suggest that the AMOC decline during the 21st century could be overestimated in these models due to the poorly resolved Labrador Current.

Increased freshwater supply to the Arctic Ocean in a warming climate makes high-latitude regions susceptible to dramatic changes in ocean circulation. As anthropogenic warming continues in the 21st century, Arctic summer sea ice is likely to disappear in a few decades[1,2], increasing the Arctic liquid freshwater storage. A stronger hydrological cycle in the atmosphere will also put more freshwater into the Arctic through an increase in net precipitation and river runoff[3,4]. Coupled climate models suggest that these extra freshwater sources to the Arctic will lead to a larger freshwater exportation to the subpolar North Atlantic in the 21st century[5,6]. The additional freshwater will increase ocean stratification and potentially slow down the Atlantic Meridional Overturning Circulation (AMOC), with serious consequences for regional and global climates[7–10].

In this study, we focus on the influence of the extra freshwater from the Arctic on the ocean circulation in the Labrador Sea, a critical region for AMOC changes[11–14]. Climate models consistently project a slowdown of the AMOC during the 21st century due to warming and freshening in the high-latitude North Atlantic[15–17]. However, the overturning and deep convection responses to freshwater input are crucially impacted by the boundary current that typically circulates around open-ocean convection regions, where deep water forms. For example, there is significant freshwater input into the Weddell Sea, a key region for bottom water formation in the Southern Ocean, due to the melting of Antarctic ice sheet and sea ice. In the presence of a well-resolved Antarctic Slope Current, the extra freshwater largely stays on the shelf region as the slope current restricts the lateral spread of freshwater, with limited influence on open-ocean convection[18]. The Labrador Current can also restrict the lateral exchange of freshwater between the shelf and open ocean[19,20]. Thus, we hypothesize that when the extra freshwater enters the Labrador Sea from the Arctic through the Canadian Arctic Archipelago[21], the Labrador Current restricts the freshwater from spreading into the open ocean and weakening the overturning circulation. Typical climate models for the Coupled Model Intercomparison Project (CMIP) of Intergoverment Panel for Climate Change (IPCC) assessment report, mostly at 1° resolution, are unable to resolve the Labrador Current[22] (supplementary Fig. 1), and thus could overestimate overturning responses to the freshwater forcing due to anthropogenic warming[23].

[1]Frontiers Science Center for Deep Ocean Multispheres and Earth System and Key Laboratory of Physical Oceanography, Ocean University of China, Qingdao, China. [2]Woods Hole Oceanographic Institution, Woods Hole, MA, USA. [3]Laoshan Laboratory, Qingdao, China. ✉e-mail: xuan.shan@whoi.edu; stsun@qnlm.ac

Here, we study the role of the Labrador Current in regulating the overturning responses to an increased Arctic freshwater export in the Labrador Sea and its influence on AMOC changes in an unprecedented high-resolution coupled simulation over the 21st century (2006–2100) under the high-emission scenario (RCP8.5) from the CMIP5 protocol. The simulation (HighRes)[24] is conducted using the Community Earth System Model version 1 (CESM1), with a nominal horizontal resolution of 0.1° for the ocean, ~6.5 km in the Labrador Sea, and 0.25° for the atmosphere (see "CESM simulations" in "Method"). HighRes performs well in reproducing the narrow Labrador Current[25] (supplementary Fig. 1) and the Labrador Sea overturning circulation[26] (supplementary Fig. 2) when compared to observations. These processes are often biased in coarse-resolution climate models (supplementary Figs. 1 and 2). To quantify the role of the Labrador Current in regulating the overturning circulation changes, we also look at the overturning responses in a coarse-resolution counterpart of HighRes, LowRes, with a nominal 1° resolution as in most climate models in CMIP5 and CMIP6. HighRes and LowRes differ from each other primarily in their horizontal resolutions. We show that the well-resolved Labrador Current in HighRes strongly restricts freshwater to the shelf and leads to a much weaker response in the Labrador Sea overturning circulation than LowRes, in which the Labrador Current is poorly resolved. Thus, we conclude that, without resolving the Labrador Current, coarse-resolution climate models may overestimate the AMOC decline during the 21st century.

Results

Increased Arctic freshwater exportation into the Labrador Sea

Consistent with climate models from CMIP6[6] and previous generations[5], HighRes projects a significant increase in liquid freshwater input to the Arctic Ocean due to anthropogenic warming (Fig. 1a–c). Under the RCP8.5 scenario in HighRes, the annual mean sea ice volume decreases by 98.5% from 16,298 km^3 in 2006–2015 to 243 km^3 in 2091–2100; summer sea ice is completely lost in the 2060s. Net precipitation and river runoff also increase significantly due to a stronger atmospheric hydrological cycle by ~161% and 39%, respectively. The larger Arctic freshwater input will necessarily lead to an increased liquid freshwater exportation into the subpolar North Atlantic, including the Labrador Sea.

We estimate the freshwater transport into the Labrador Sea (Fig. 1d) from the north across Davis Strait, from the west across Hudson Strait, and from the east by the West Greenland Current in HighRes (see "Freshwater flux" in "Method"). Salinity averaged in the Labrador Sea (denoted by the box in Fig. 1d) in the year 2006 is used as the reference salinity. The increase in the freshwater flux from Davis Strait is most significant, at a rate of about 1.4 mSv yr^{-1} over the 21st century (Fig. 1e). The freshwater flux across Hudson Strait also enhances with a smaller rate of 0.35 mSv yr^{-1} (Fig. 1e). Both the trends are significant at the 95% confidence level according to a two-tailed Student' *t* test. The freshwater flux coming from the east weakly increases in 2020–2040 and decreases after the year 2040 (Fig. 1f). The freshwater pathway into the Labrador Sea is determined by several processes, including the Arctic circulation and the location of freshwater sources. The differing freshwater flux trends between the western and the eastern routes are likely related to the structure of liquid freshwater increases in the Arctic Ocean in HighRes: liquid freshwater content increases in the Canadian basin but decreases in the Eurasian basin (supplementary Fig. 3).

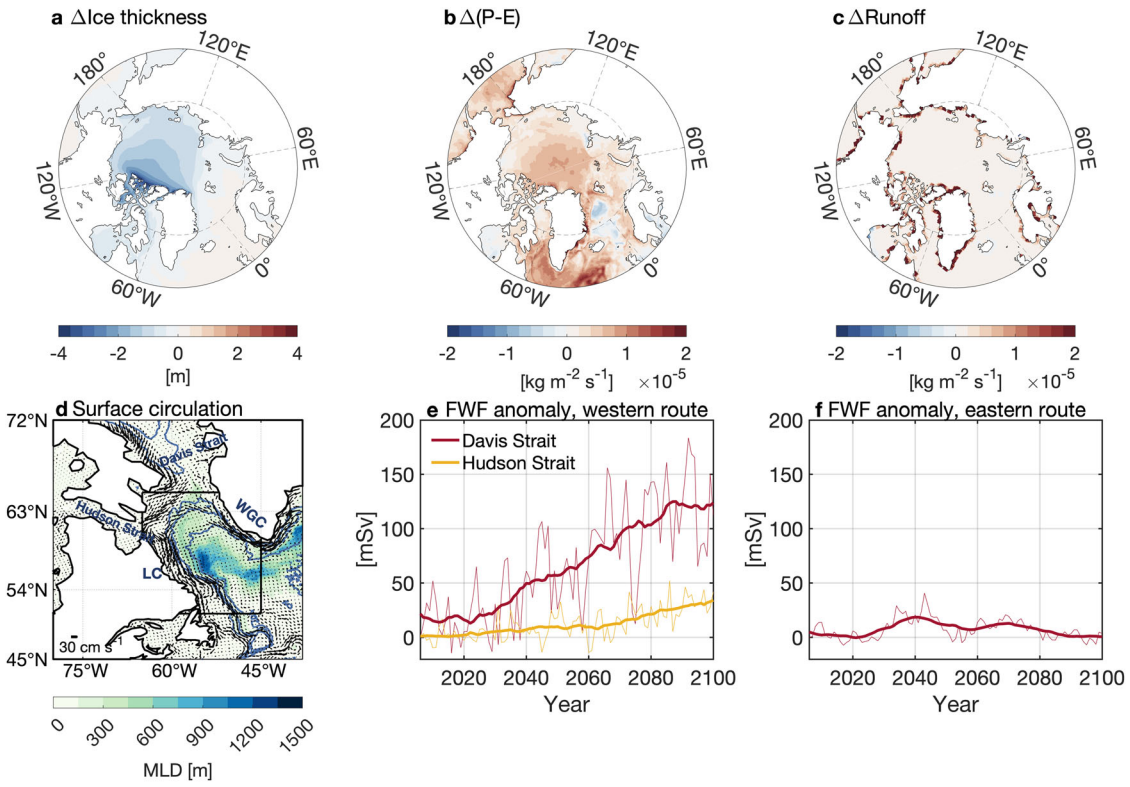

Fig. 1 | Enhanced freshwater input into the Arctic Ocean and freshwater exportation into the Labrador Sea. Changes (2091–2100 minus 2006–2015) in **a** equivalent sea-ice thickness, **b** precipitation minus evaporation (P-E), and **c** river runoff in the Arctic in HighRes. **d** Surface ocean circulation in the Labrador Sea in HighRes over 2006–2015. The shading shows mixed layer depth in March during the same period. The 1000 m, 2000 m, and 3000 m isobaths are indicated by blue contours. The black box encloses the Labrador Sea region. LC is the Labrador Current. WGC is the West Greenland Current. Time series of anomalous freshwater flux (FWF) into the Labrador Sea (defined as positive) from **e** the west of Greenland across Davis Strait (red line) and Hudson Strait (yellow line) and **f** from the east of Greenland. The freshwater flux anomaly is relative to the year 2006. The thin lines in **e** and **f** show the annual mean anomaly. The thick lines represent 20-year running mean.

https://doi.org/10.1038/s41467-024-51449-9

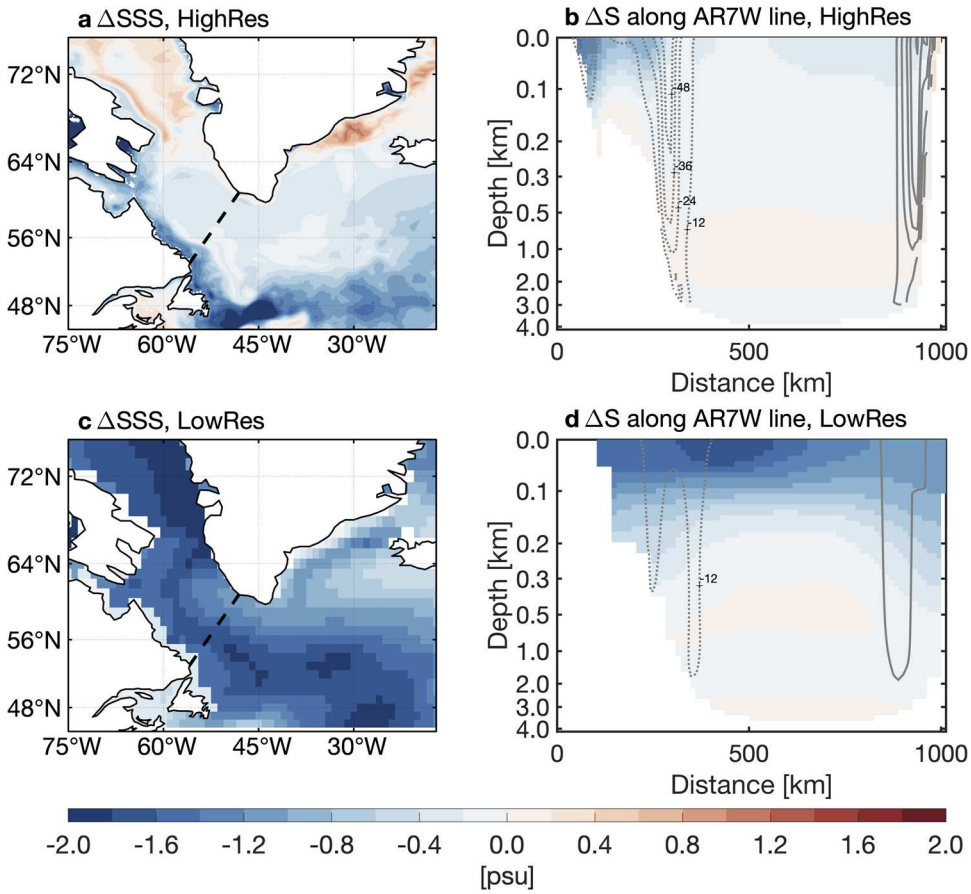

Fig. 2 | Freshening of the Labrador Sea during the 21st century. a, **c** Changes (2091–2100 minus 2006–2015) in sea surface salinity (SSS) in **a** HighRes and **c** LowRes. The black dashed line indicates the Atlantic Repeat Hydrography Line 7 West line (AR7W line). **b**, **d** Salinity changes (2091–2100 minus 2006–2015) along the AR7W line in **b** HighRes and **d** LowRes. The contour lines show velocity of currents across the AR7W line with interval of 12 cm s^{-1}. The dashed (solid) lines represent currents out of (into) the Labrador Sea.

Surface freshening confined to the western shelf by the Labrador Current

The extra freshwater in the Labrador Sea reduces sea surface salinity, but the freshening is mostly confined to the shelf close to Newfoundland and Labrador of Canada (Fig. 2a). The freshening on the shelf is ~0.67 psu in 2091–2100 relative to 2006–2015. In contrast, in the interior Labrador Sea with depth deeper than 2000 m, where deep convection occurs, the surface freshening is only ~0.27 psu. We quantify the salinity changes along the Atlantic Repeat Hydrography Line 7 West line (AR7W line)[25] (black dashed line in Fig. 2a). The freshening is most obvious in the upper 150 m on the shelf (Fig. 2b). The exchange of freshwater between the shelf and the open ocean is strongly restricted by the narrow Labrador Current (Fig. 2b, supplementary Fig. 1), consistent with previous studies[19,20]. The Labrador Current may also help flush the freshwater out into the subpolar North Atlantic, contributing to reducing the freshening effects. Coarse-resolution models (e.g., LowRes), on the other hand, cannot fully resolve the Labrador Current, and thus may misrepresent the freshening of the interior Labrador Sea with excessive freshwater input from the shelf. Indeed, with similar increase in total freshwater flux that is mostly due to enhanced freshwater flux from the western route via Davis Strait and Hudson Strait (supplementary Fig. 4), the surface freshening is almost uniform in the Labrador Sea in LowRes, with a 1.52 psu decrease in the interior (Fig. 2c). The broader surface salinity decrease is related to the too weak and wide Labrador Current (Fig. 2d, supplementary Fig. 1), which allows freshwater to enter the interior Labrador Sea. Thus, we suggest that the coarse-resolution CESM model overestimates the freshwater influence on surface salinity changes in the Labrador Sea.

The Labrador Current also regulates ocean stratification and mixed layer depth (MLD) changes in the interior Labrador Sea due to surface freshening. Ocean stratification, quantified as the density difference between the sea surface and 1 km depth, increases by 91% from 2006–2015 to 2091–2100 in HighRes (supplementary Fig. 5). The strengthening is surface intensified and almost equally attributed to surface warming and freshening (Fig. 3a, b, supplementary Fig. 6). In contrast with HighRes, the upper-ocean stratification increases more dramatically in the 21st century by 158% in LowRes (supplementary Fig. 5). The larger stratification increase in LowRes can be mostly (~80%) attributed to the widespread surface freshening in the Labrador Sea that leads to a dramatic decrease in surface density (Fig. 3c, d, supplementary Fig. 6). Similar conclusions can be drawn for MLD changes (supplementary Fig. 7). In HighRes, the March MLD in the interior Labrador Sea decreases by 56% from 430 m in 2006–2015 to 190 m in 2091–2100. While in LowRes, the March MLD shoals by 91% from 928 m to 83 m during the same period. We note that the present-day MLD in LowRes is overestimated as in many coarse-resolution models[27–29]. The results highlight the role of the Labrador Current in future ocean stratification changes in the Labrador Sea and suggest that coarse-resolution models may overestimate the stratification increase due to freshwater forcing.

Response of the Labrador Sea overturning and the AMOC

Through its impacts on surface freshening and stratification changes, the Labrador Current regulates overturning circulation changes in a

https://doi.org/10.1038/s41467-024-51449-9

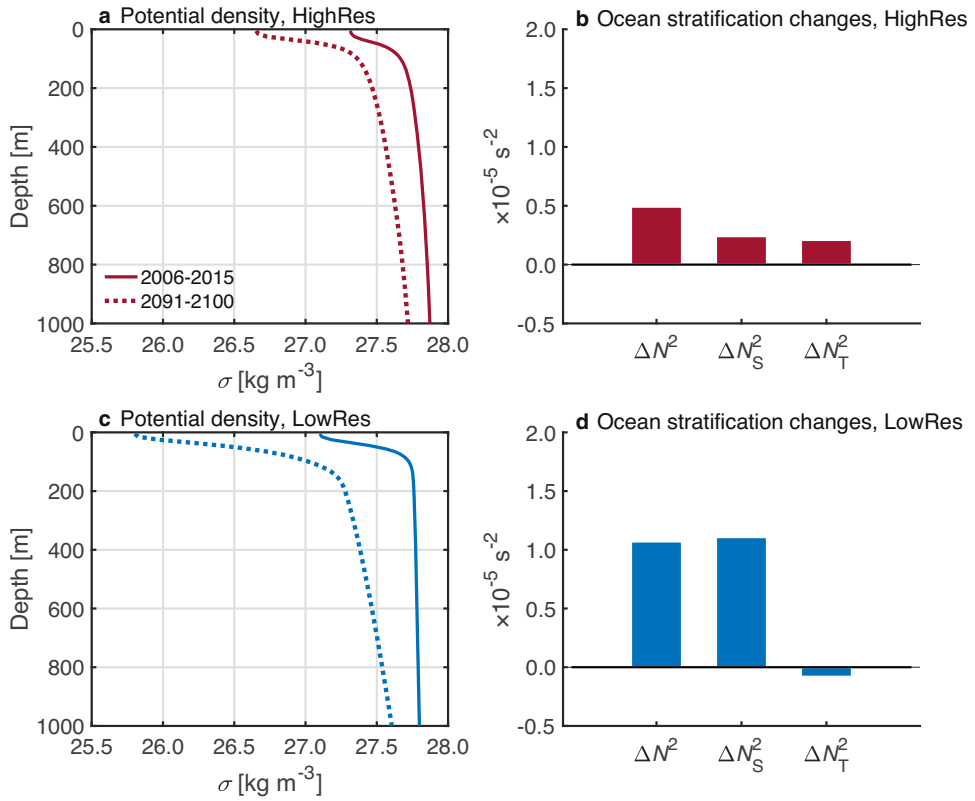

Fig. 3 | Strengthening of ocean stratification in the interior Labrador Sea. **a**, **c** Changes of potential density (σ, reference pressure at sea surface) profiles in the Labrador Sea in **a** HighRes and **c** LowRes. Solid (dashed) lines indicate the mean in 2006–2015 (2091–2100). **b**, **d** Strengthening of the upper-1000 m ocean stratification, N^2, calculated as $g/\sigma^{1000\,m}\cdot(\sigma^{1000\,m}-\sigma^{0m})/1000$ and its contributions due to temperature changes, ΔN_T^2, and salinity changes, ΔN_S^2, in **b** HighRes and **d** LowRes. The temperature stratification, N_T^2, is calculated as $-g\alpha^{500m}(T^{1000\,m}-T^{0m})/1000$, where T is the potential temperature and α is the thermal expansion coefficient. The haline stratification, N_S^2, is calculated as $g\beta^{500m}(S^{1000\,m}-S^{0m})/1000$, where S is salinity and β is the haline contraction coefficient. Only regions in the Labrador Sea (denoted by the box in Fig. 1d) deeper than 2000 m are considered here.

warming climate. The stratification increase will decrease deep water formation in the Labrador Sea and potentially contribute to the AMOC weakening during the 21st century. We quantify the Labrador Sea overturning at the west leg of Overturning in the Subpolar North Atlantic Program (OSNAP) observing system (Fig. 4a, c, see "OSNAP overturning streamfunction" in "Method"), at the exit of the Labrador Sea. The Labrador Sea overturning is weakened by ~55% in HighRes from 2006–2015 to 2091–2100. In comparison, the weakening of the Labrador Sea overturning in LowRes is more substantial by ~ 90% during the same period. The deep convection in LowRes almost completely shuts down at the end of the 21st century. The much stronger weakening of the Labrador Sea overturning in LowRes can be attributed to the overly stratified ocean in the Labrador Sea. We calculate the surface water mass transformation (SWMT), which is dynamically connected to the overturning[13,14,30], using surface buoyancy flux and surface density (see "Surface water mass transformation" in "Methods" section). The SWMT largely reproduces the Labrador Sea overturning circulation as well as its changes during the 21st century (supplementary Fig. 8). Decomposing the SWMT changes into contributions due to changes in the surface buoyancy flux and surface density (see "Surface water mass transformation" in "Method"), we show that the differing Labrador Sea overturning responses between HighRes and LowRes are mainly owing to changes in surface density structure (supplementary Fig. 8). The surface buoyancy flux is not significantly different between HighRes and LowRes at 98% confidence level (supplementary Fig. 9) and cannot explain their difference in the overturning changes.

The weakening of the Labrador Sea overturning circulation contributes to the AMOC decline during the 21st century. We calculate the North Atlantic overturning in density space and then remap it to depth space following previous studies[31,32] (see "Density-space AMOC" in "Method", supplementary Fig. 10). Consistent with the Labrador Sea overturning circulation changes, the AMOC decline appears to be faster in LowRes (Fig. 4d) than HighRes (Fig. 4b). Overturning changes across OSNAP East, which dominates the North Atlantic overturning in observations, may also contribute to the faster AMOC decline in LowRes (supplementary Figs. 11 and 12). However, the difference in OSNAP East overturning changes between LowRes (53%) and HighRes (39%) is less dramatic as compared to OSNAP West (Fig. 4a, c).

Discussion

In this study, we highlight the role of the Labrador Current in regulating the Labrador Sea responses to increased liquid freshwater input due to anthropogenic warming. The narrow Labrador Current strongly restricts the lateral exchange of freshwater between the continental shelf and open ocean. In the absence of this narrow boundary current, the extra freshwater input from the Arctic spreads into the open ocean and causes a much stronger increase in ocean stratification, leading to an overestimated weakening of the Labrador Sea overturning circulation. The impact of the Labrador Current in restricting lateral freshwater exchange might evolve as the climate continues to warm. HighRes predicts a weakening of the Labrador Current due to surface wind changes (supplementary Fig. 13), suggesting a slightly diminishing role of the Labrador Current in the future climate. Nevertheless, given that the Labrador Sea overturning circulation makes a significant contribution to the AMOC in many climate models of coarse resolution[27–29], our results suggest that the AMOC weakening may be overestimated in these climate models.

https://doi.org/10.1038/s41467-024-51449-9

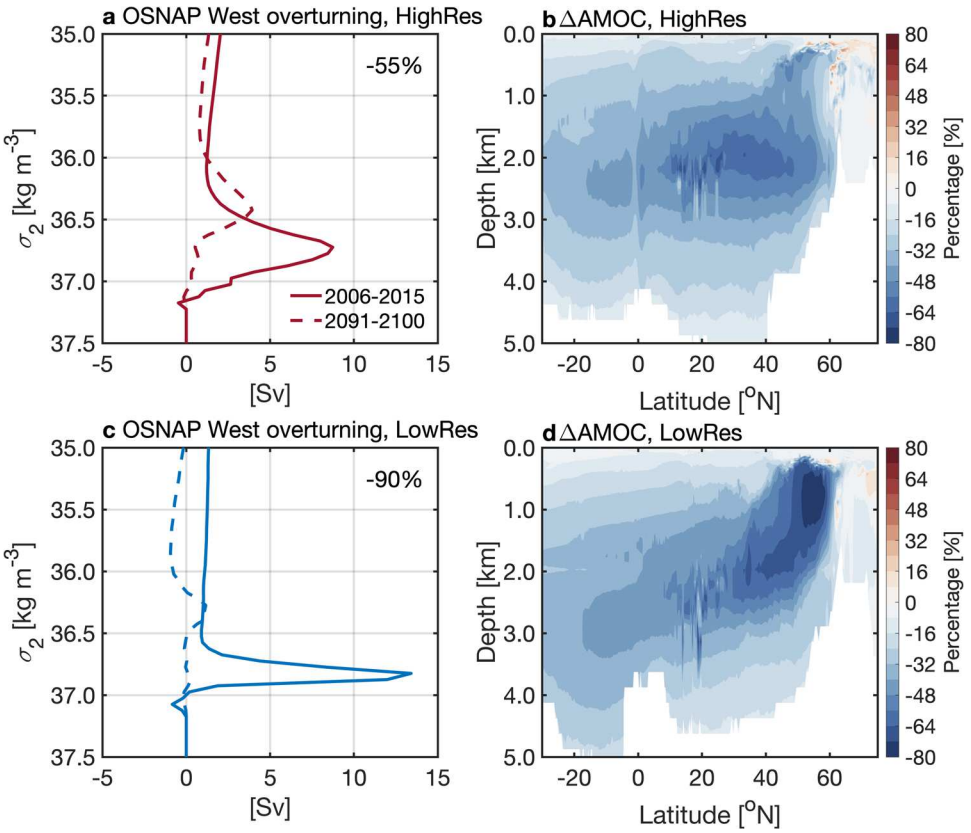

Fig. 4 | Weakening of Labrador Sea overturning and the Atlantic Meridional overturning circulation (AMOC). a, **c** Changes of overturning across the west leg of Overturning in the Subpolar North Atlantic Program observing system (OSNAP West) in **a** HighRes and **c** LowRes. Solid (dashed) lines indicate the mean in 2006–2015 (2091–2100). The percentage changes in the maximum overturning streamfunction between 2006–2015 and 2091–2100 is denoted on the upper-right corner in **a** and **c**. **b**, **d** Percentage changes in the AMOC from 2006–2015 to 2091–2100 in **b** HighRes and **d** LowRes. The percentage changes are calculated as the AMOC streamfunction differences between 2091–2100 and 2006–2015, divided by the maximum AMOC at 40°N in 2006–2015 in each simulation. The AMOC is calculated in density space and then remapped into depth space using the time and zonal mean depth of each density layer.

A similar dependence of the AMOC decline rate on model resolutions has been found in GFDL models[33]. However, the overturning responses to anthropogenic forcing are complex and involve many processes (e.g., ice sheet melting) that are not resolved even in the high-resolution CESM. Our discussions are mostly based on one single climate model under the previous CMIP5 protocol. It is possible that the dependence of the AMOC decline rate on model resolution is model-dependent. In this regard, HighResMIP[34] may be useful for a more comprehensive comparison of AMOC decline among various climate models. However, the high-resolution models in HighResMIP, mostly based on NEMO ocean model[35,36], only partially resolve the boundary current at 0.25° resolution and simulate the climate until year 2050, beyond which the AMOC decline is more significant[15,16]. High-resolution projections with various model configurations until 2100 are highly desired to validate our results and enable a more comprehensive understanding of the AMOC changes during the 21st century.

As anthropogenic warming continues, more freshwater is expected to enter the subpolar North Atlantic from the Greenland ice sheet melting and Arctic freshwater release. The extra freshwater input will necessarily interact with deep convection and cause a slowdown of the AMOC[37–39]. However, our results suggest that future AMOC responses will be sensitive to how the extra freshwater input is distributed in the high-latitude regions. To address this question, we need to monitor the freshwater sources and their exportation pathways through Arctic-subpolar North Atlantic gateways towards regions that could impact the AMOC. High-resolution models are also desired for a more accurate representation of freshwater transports associated with narrow boundary currents[40–43] and oceanic eddies[44–47] that are not resolved in coarse-resolution models.

Methods

CESM simulations

The simulations used in this paper were carried out by CESM1.3 at the International Laboratory for High-Resolution Earth System Prediction (iHESP)[24]. CESM comprises the Community Atmosphere Model version 5 (CAM5), the Parallel Ocean Program version 2 (POP2), the Community Ice Code version 4 (CICE4), and the Community Land Model version 4 (CLM4). We make use of the configuration with high and low model horizontal resolutions. For HighRes, the resolutions of atmosphere, ocean, and sea-ice components are 0.25°, 0.1°, and 0.1°, respectively. For LowRes, the nominal horizontal resolutions are 1°. Both CESM simulations were run under the representative concentration pathway 8.5 (RCP8.5) forcing from 2006 to 2100 in accordance with the CMIP5 experimental protocol.

Freshwater flux

The freshwater flux (FWF) is defined as follows

$$\mathrm{FWF}(x,y,z,t) = v(x,y,z,t) \cdot \frac{S_{\mathrm{ref}} - S(x,y,z,t)}{S_{\mathrm{ref}}} dA \qquad (1)$$

where v is the cross-section velocity (in units of $\mathrm{m\,s^{-1}}$), S is the salinity (in units of psu), dA is the cross-section area at each grid

point (in units of m^2), S_{ref} is the reference salinity which is set as the salinity averaged in the Labrador Sea (denoted by the box in Fig. 1d) in the year 2006. The S_{ref} is similar in the two simulations with 34.7 psu (34.8 psu) for HighRes (LowRes). The time series of freshwater flux into the Labrador Sea shown in Fig. 1 and supplementary Fig. 4 is computed by summing up annual FWF at grid points with $S < S_{ref}$ and currents into the Labrador Sea along each section denoted in Fig. 1d. The unit of FWF is converted from $m^3\,s^{-1}$ to mSv ($1\,mSv = 10^3\,m^3\,s^{-1}$) in this paper.

OSNAP overturning streamfunction

Dense waters that reside in the lower limb of the AMOC are produced mainly in the eastern subpolar North Atlantic (i.e., the Irminger and Iceland basins) in observations, and to a lesser extent, in the western subpolar North Atlantic (i.e., the Labrador Sea)[48]. The strength of dense water formation can be measured by overturning across OSNAP West and OSNAP East in density space. In this paper, OSNAP overturning is calculated in density space with the density referenced to 2000-m depth (σ_2) as the vertical coordinate (in units of $kg\,m^{-3}$, after subtracting $1000\,kg\,m^{-3}$). Volume fluxes are integrated from west to east and from higher to lower density.

Surface water mass transformation

The overturning streamfunction in the subpolar North Atlantic and its low-frequency variability are largely determined by the SWMT[13,14,30]. The SWMT is the transformation of water from one density class to another due to buoyancy losses and gains at the sea surface. The SWMT is calculated by integrating the surface density flux over outcrop regions in each density bin as follows

$$\mathrm{SWMT}(\sigma_2) = \frac{1}{\Delta\sigma_2}\int\int B dA \tag{2}$$

where B is the surface density flux (in units of kg seawater $m^{-2}\,s^{-1}$, defined as positive for ocean density increase), σ_2 is the density referenced to 2000-m depth (in units of $kg\,m^{-3}$, after subtracting $1000\,kg\,m^{-3}$), dA is the surface outcrop area (in units of m^2, corresponding to densities in the range from σ_2-$\Delta\sigma_2/2$ to $\sigma_2 + \Delta\sigma_2/2$). The unit of SWMT is converted from $m^3\,s^{-1}$ to Sv ($1\,Sv = 10^6\,m^3\,s^{-1}$) in the paper. The density flux comprises heat and salt fluxes that referred to as B_{heat} and B_{salt}, respectively. The heat flux is

$$B_{heat} = -\frac{\alpha}{C_p}Q \tag{3}$$

where α is the thermal expansion coefficient (in units of K^{-1}), C_p is the specific heat capacity of seawater (in units of $J\,kg^{-1}\,K^{-1}$), Q is the surface net heat flux (in units of $W\,m^{-2}$, defined as positive for ocean heat gain), which is the sum of surface radiation and turbulent heat fluxes. The salt flux is

$$B_{salt} = -\beta\frac{S}{1-S}F \tag{4}$$

where S is the sea surface salinity (in units of msu, $1\,msu = 10^{-3}\,psu$), β is the haline contraction coefficient (in units of msu^{-1}), and F is the surface freshwater flux (in units of kg freshwater $m^{-2}\,s^{-1}$, defined as negative for ocean salinity increase).

Variations in SWMT can be decomposed into contributions due to changes in surface density flux and surface density. We calculate the latter (referred to as $\mathrm{SWMT_{OCN}}$) in this paper by replacing the time-dependent surface density flux with the monthly-mean surface density flux in 2006 in Eq. (2).

Density-space AMOC

We calculate the AMOC in density space that better represents the overturning circulation at high latitudes. The AMOC streamfunction is defined as follows

$$\mathrm{AMOC}(y,\sigma,t) = -\int_{z_{bot}}^{0}\int_{x_w}^{x_e} H(\sigma'(x,y,z,t)-\sigma)v(x,y,z,t)dxdz \tag{5}$$

where H is the Heaviside function, σ' represents the density field, x is longitude, y is latitude, z is depth, t is time, σ is the density at which the streamfunction is calculated, and v is the Meridional velocity. The zonal integral is performed across the Atlantic Ocean from the western boundary (x_w) to the eastern boundary (x_e), and the vertical integral is performed from the ocean bottom (z_{bot}) to the sea surface. Density referenced to 2000-m depth (σ_2) is used as the vertical coordinate (in units of $kg\,m^{-3}$, after subtracting $1000\,kg\,m^{-3}$). We also remap the AMOC streamfunction in density space into depth space using the time and zonally averaged depth of each density layer following previous studies[31,32].

Data availability

The climate model simulations and observation data used in this study are publicly available and can be downloaded from the following websites: CESM model outputs (https://ihesp.github.io/archive/products/ihesp-products/data-release/DataRelease_Phase2.html or http://ihesp.qnlm.ac), OSNAP overturning (https://www.o-snap.org/). The data generated in this study for plotting the figures in the paper are available from https://doi.org/10.5281/zenodo.12249262.

Code availability

The iHESP version of CESM HighRes code is available at ZENODO via https://doi.org/10.5281/zenodo.3637771. The codes used to generate the figures in the paper can be accessed at https://doi.org/10.5281/zenodo.12249262. The Matlab2022b is used for plotting.

References

1. Notz, D. & Community, S. Arctic sea ice in CMIP6. *Geophys. Res. Lett.* **47**, e2019GL086749 (2020).
2. Kim, Y.-H., Min, S.-K., Gillett, N. P., Notz, D. & Malinina, E. Observationally-constrained projections of an ice-free Arctic even under a low emission scenario. *Nat. Commun.* **14**, 3139 (2023).
3. Bintanja, R. & Selten, F. M. Future increases in Arctic precipitation linked to local evaporation and sea-ice retreat. *Nature* **509**, 479–482 (2014).
4. Vihma, T. et al. The atmospheric role in the Arctic water cycle: a review on processes, past and future changes, and their impacts. *J. Geophys. Res. Biogeosci.* **121**, 586–620 (2016).
5. Haine, T. W. N. et al. Arctic freshwater export: status, mechanisms, and prospects. *Glob. Planet. Change* **125**, 13–35 (2015).
6. Wang, Q. et al. A review of Arctic–Subarctic ocean linkages: past changes, mechanisms, and future projections. *Ocean-Land-Atmos. Res.* **2**, 0013 (2023).
7. Vellinga, M. & Wood, R. A. Global climatic impacts of a collapse of the Atlantic thermohaline circulation. *Clim. Change* **54**, 251–267 (2002).
8. Cheng, W., Bitz, C. M. & Chiang, J. C. H. Adjustment of the global climate to an abrupt slowdown of the Atlantic meridional overturning circulation. *Geophys. Monogr. Ser.* **173**, 295 (2007).
9. Woollings, T., Gregory, J. M., Pinto, J. G., Reyers, M. & Brayshaw, D. J. Response of the North Atlantic storm track to climate change shaped by ocean–atmosphere coupling. *Nat. Geosci.* **5**, 313–317 (2012).
10. Bellomo, K., Angeloni, M., Corti, S. & Von Hardenberg, J. Future climate change shaped by inter-model differences in Atlantic

meridional overturning circulation response. *Nat. Commun.* **12**, 3659 (2021).
11. Jackson, L. C., Peterson, K. A., Roberts, C. D. & Wood, R. A. Recent slowing of Atlantic overturning circulation as a recovery from earlier strengthening. *Nat. Geosci.* **9**, 518–522 (2016).
12. Thornalley, D. J. R. et al. Anomalously weak Labrador Sea convection and Atlantic overturning during the past 150 years. *Nature* **556**, 227–230 (2018).
13. Yeager, S. et al. An outsized role for the Labrador Sea in the multidecadal variability of the Atlantic overturning circulation. *Sci. Adv.* **7**, eabh3592 (2021).
14. Oldenburg, D., Wills, R. C. J., Armour, K. C., Thompson, L. & Jackson, L. C. Mechanisms of low-frequency variability in North Atlantic ocean heat transport and AMOC. *J. Clim.* **34**, 4733–4755 (2021).
15. Cheng, W., Chiang, J. C. H. & Zhang, D. Atlantic Meridional overturning circulation (AMOC) in CMIP5 models: RCP and historical simulations. *J. Clim.* **26**, 7187–7197 (2013).
16. Weijer, W., Cheng, W., Garuba, O. A., Hu, A. & Nadiga, B. T. CMIP6 models predict significant 21st century decline of the Atlantic Meridional overturning circulation. *Geophys. Res. Lett.* **47**, e2019GL086075 (2020).
17. Climate Change 2021: the physical science basis. Working Group I Contribution to the Sixth Assessment. https://www.ipcc.ch/report/sixth-assessment-report-working-group-i/, Cambridge University Press (2023).
18. Lockwood, J. W., Dufour, C. O., Griffies, S. M. & Winton, M. On the role of the Antarctic slope front on the occurrence of the Weddell Sea polynya under climate change. *J. Clim.* **34**, 2529–2548 (2021).
19. Myers, P. G. Impact of freshwater from the Canadian Arctic Archipelago on Labrador Sea Water formation. *Geophys. Res. Lett.* **32**, 2004GL022082 (2005).
20. Houssais, M. -N. & Herbaut, C. Atmospheric forcing on the Canadian Arctic Archipelago freshwater outflow and implications for the Labrador Sea variability. *J. Geophys. Res.* **116**, C00D02 (2011).
21. Zhang, J. et al. Labrador Sea freshening linked to Beaufort Gyre freshwater release. *Nat. Commun.* **12**, 1229 (2021).
22. Talandier, C. Improvements of simulated Western North Atlantic current system and impacts on the AMOC. *Ocean Model.* **76**, 1–19 (2014).
23. He, F. & Clark, P. U. Freshwater forcing of the Atlantic Meridional overturning circulation revisited. *Nat. Clim. Chang.* **12**, 449–454 (2022).
24. Chang, P. et al. An unprecedented set of high-resolution earth system simulations for understanding multiscale interactions in climate variability and change. *J. Adv. Model. Earth Syst.* **12**, e2020MS002298 (2020).
25. Pickart, R. S. & Spall, M. A. Impact of Labrador Sea convection on the North Atlantic meridional overturning circulation. *J. Phys. Oceanogr.* **37**, 2207–2227 (2007).
26. Fu, Y. et al. Seasonality of the Meridional overturning circulation in the subpolar North Atlantic. *Commun. Earth Environ.* **4**, 181 (2023).
27. Danabasoglu, D. et al. North Atlantic simulations in coordinated ocean-ice reference experiments phase II (CORE-II). Part I: mean states. *Ocean Model.* **73**, 76–107 (2014).
28. Heuzé, C. North Atlantic deep water formation and AMOC in CMIP5 models. *Ocean Sci.* **13**, 609–622 (2017).
29. Li, F. et al. Local and downstream relationships between Labrador Sea Water volume and North Atlantic Meridional overturning circulation variability. *J. Clim.* **32**, 3883–3898 (2019).
30. Jackson, L. C. & Petit, T. North Atlantic overturning and water mass transformation in CMIP6 models. *Clim. Dyn.* **60**, 2871–2891 (2023).
31. Xu, X., Rhines, P. B. & Chassignet, E. P. On mapping the diapycnal water mass transformation of the upper North Atlantic Ocean. *J. Phys. Oceanogr.* **48**, 2233–2258 (2018).
32. Rousselet, L., Cessi, P. & Forget, G. Routes of the upper branch of the Atlantic Meridional overturning circulation according to an ocean state estimate. *Geophys. Res. Lett.* **47**, e2020GL089137 (2020).
33. Delworth, T. L. et al. Simulated climate and climate change in the GFDL CM2.5 high-resolution coupled climate model. *J. Clim.* **25**, 2755–2781 (2012).
34. Roberts, M. J. et al. Sensitivity of the Atlantic Meridional overturning circulation to model resolution in CMIP6 HighResMIP simulations and implications for future changes. *J. Adv. Model. Earth Syst.* **12**, e2019MS002014 (2020).
35. Jackson, L. C. et al. Impact of ocean resolution and mean state on the rate of AMOC weakening. *Clim. Dyn.* **55**, 1711–1732 (2020).
36. Koenigk, T. et al. Deep mixed ocean volume in the Labrador Sea in HighResMIP models. *Clim. Dyn.* **57**, 1895–1918 (2021).
37. Rahmstorf, S. et al. Exceptional twentieth-century slowdown in Atlantic Ocean overturning circulation. *Nat. Clim. Change* **5**, 475–480 (2015).
38. Böning, C. W., Behrens, E., Biastoch, A., Getzlaff, K. & Bamber, J. L. Emerging impact of Greenland meltwater on deepwater formation in the North Atlantic Ocean. *Nat. Geosci.* **9**, 523–527 (2016).
39. Yang, Q. et al. Recent increases in Arctic freshwater flux affects Labrador Sea convection and Atlantic overturning circulation. *Nat. Commun.* **7**, 10525 (2016).
40. Gillard, L. C., Hu, X., Myers, P. G. & Bamber, J. L. Meltwater pathways from marine terminating glaciers of the Greenland ice sheet. *Geophys. Res. Lett.* **43**, 10,873–10,882 (2016).
41. Luo, H. et al. Oceanic transport of surface meltwater from the southern Greenland ice sheet. *Nat. Geosci.* **9**, 528–532 (2016).
42. Wang, H., Legg, S. & Hallberg, R. The effect of Arctic freshwater pathways on North Atlantic convection and the Atlantic Meridional overturning circulation. *J. Clim.* **31**, 5165–5188 (2018).
43. Spall, M. A., Semper, S. & Vage, K. Mechanisms of offshore solid and liquid freshwater flux from the East Greenland current. *J. Phys. Oceanogr.* **54**, 379–397 (2024).
44. Schmidt, S. & Send, U. Origin and composition of seasonal Labrador Sea. *Freshw. J. Phys. Oceanogr.* **37**, 1445–1454 (2007).
45. McGeehan, T. & Maslowski, W. Impact of shelf–basin freshwater transport on deep convection in the western Labrador Sea. *J. Phys. Oceanogr.* **41**, 2187–2210 (2011).
46. Weijer, W., Maltrud, M. E., Hecht, M. W., Dijkstra, H. A. & Kliphuis, M. A. Response of the Atlantic Ocean circulation to Greenland Ice Sheet melting in a strongly-eddying ocean model. *Geophys. Res. Lett.* **39**, L09606 (2012).
47. Rieck, J. K., Böning, C. W. & Getzlaff, K. The nature of eddy kinetic energy in the Labrador sea: different types of mesoscale eddies, their temporal variability, and impact on deep convection. *J. Phys. Oceanogr.* **49**, 2075–2094 (2019).
48. Lozier, M. S. et al. A sea change in our view of overturning in the subpolar North Atlantic. *Science* **363**, 516–521 (2019).

Acknowledgements

Funding: National Science Foundation Grant OPP-2211691 (to M.S.), Ocean University of China Fellowship for International Postdoctoral Research (to X.S.).

Author contributions

Conceptualization: S.S., L.W. Investigation: X.S. Visualization: X.S. Supervision: S.S., L.W. Writing—original draft: X.S. Writing—review & editing: S.S., L.W., M.S.

Competing interests

The authors declare no competing interests.

Additional information

Supplementary information The online version contains supplementary material available at https://doi.org/10.1038/s41467-024-51449-9.

Correspondence and requests for materials should be addressed to Xuan Shan or Shantong Sun.

Peer review information *Nature Communications* thanks Virna Meccia and the other, anonymous, reviewer for their contribution to the peer review of this work. A peer review file is available.